

Projective Ponzano–Regge spin networks and their symmetries

Vincenzo Aquilanti¹, Annalisa Marzuoli^{2,3}

¹ Dipartimento di Chimica, Biologia e Biotecnologie, via Elce di Sotto 8, Università di Perugia, 06123 Perugia, I

² Dipartimento di Matematica ‘F. Casorati’, Università degli Studi di Pavia, via Ferrata 1, 27100 Pavia, I

³ INFN, Sezione di Pavia, via Bassi 6, 27100 Pavia, I

E-mail: annalisa.marzuoli@unipv.it

Abstract. We present a novel hierarchical construction of projective spin networks of the Ponzano–Regge type from an assembling of five quadrangles up to the combinatorial 4-simplex compatible with a geometrical realization in Euclidean 4-space. The key ingredients are the projective Desargues configuration and the incidence structure given by its space-dual, on the one hand, and the Biedenharn–Elliott identity for the $6j$ symbol of $SU(2)$, on the other. The interplay between projective-combinatorial and algebraic features relies on the recoupling theory of angular momenta, an approach to discrete quantum gravity models carried out successfully over the last few decades. The role of Regge symmetry –an intriguing discrete symmetry of the $6j$ which goes beyond the standard tetrahedral symmetry of this symbol– will be also discussed in brief to highlight its role in providing a natural regularization of projective spin networks that somehow mimics the standard regularization through a q -deformation of $SU(2)$.

1. Introduction

The Hilbert system of axioms for an incidence geometry deals with ideal elements such as points, lines and planes, together with the notion of concurrence (incidence) relations [1, 2]. The resulting pre-metric admissible configurations can be also studied as concrete (finite) sets of points, lines and planes in specific geometries, the Euclidean, affine and projective planes or their higher-dimensional counterparts: one then speaks of *realizations* of some given incidence configuration. The simplest abstract incidence structures have been exploited in the (re)coupling theory of $SU(2)$ angular momentum since the earliest times of Fano and Racah [3] and, more in general, combinatorial methods have been widely applied to the study of discretized quantum spacetimes since the seminal contributions of Giorgio Ponzano and Tullio Regge [4] and Roger Penrose [5]. ‘Quantum spin networks’, a term that nowadays includes quite a wide range of interlaced research fields –from basic features and applications of quantum field theories in low dimensions [6, 7], up to the ‘Loop’ approaches to the quantization of General Relativity [8, 9]– will be shown to emerge solely from the basic axioms and theorems of finite-dimensional projective geometry suitably combined with quantum angular momentum theory as rooted in the diagrammatic formalism of Yutsis graphs [10] (a self-contained account on projective configurations and diagrammatic-combinatorial tools is collected in two appendices).

The combinatorial–projective structures emerging from the hierarchical construction carried out in section 2 are interpreted as associated with collective modes of elementary ‘quantum geometries’ on the gravitational side [11, 12, 13, 14], and as related to integrable quantum many-body systems of interest also in atomic and molecular physics [15, 16, 17], on the other. We recognize in particular that –starting from the $6j$ symbol of $SU(2)$ encoded into a quadrangle associated with the projective configuration of four points joined in pairs by six distinct lines– a recollection of five nested quadrangles is projectively nothing but the Desargue configuration $(10)_3$ (ten points and ten lines, with each of its ten points incident to three lines and each of its ten lines incident to three points). We will show how such a configuration can be consistently labeled with $SU(2)$ spin variables as to comply with the algebraic content of the Biedenharn–Elliot (BE) identity treated in section 2. Moreover: *i*) Desargues configuration can be realized in a 3D Euclidean space, a well known fact ensured by Desargues’ theorem which holds true in any dimension > 2 , see appendix 5.2; *ii*) according to the basic axioms of projective geometry, each theorem must be valid under projective dualities, to be meant as either the usual (point \leftrightarrow line) exchanges in the plane realization or as (point \leftrightarrow plane) and (line \leftrightarrow line) exchanges when viewed in 3D space. On the basis of the above remarks we will remind first how the ‘space–dual’ of Desargues configuration has a combinatorial content that matches to the realization of an Euclidean 4-simplex (bounded by five tetrahedra) and then we will provide the natural $SU(2)$ labeling of its edges. This result is relevant for all Ponzano–Regge-like quantum gravity models proposed over the years [18], since it would explain the apparent dichotomy in the assignment of spin labels to triads of angular momenta: in Yutsis-type diagrams (and in most models used in Loop quantum gravity) the correspondence is (triad) \rightarrow (3-valent vertex), while in Ponzano–Regge and other approaches [11] it is assumed that (triad) \rightarrow (triangular faces) (*cf.* appendix 5.1). Actually both correspondences are fully consistent in 3D Euclidean space because they are related by Poincaré 2D duality for polyhedra, and the tetrahedron is obviously self–dual in this sense. However, if we keep on assuming, much in the spirit of Regge Calculus [19], the prominent role of the assignment (edge length) \rightarrow (spin label), then the 4-simplex Desargue spin network automatically complies with this requirement and inherits triangular inequalities on triangular faces just as a consequence of the projective dualization procedure. (Recall that in the Euclidean path integral formulation of Regge–discretized gravity the measure is expressed in terms of edge lengths, the discrete analog of the functional measure over metrics, the latter being the dynamical variables of General Relativity). In the final part of section 2 we will briefly comment on the issues of dimensional reduction and increase in this upgraded projective context.

In section 3 the association between the Desargues configuration and the Biedenharn–Elliot identity for the $6j$ symbol will be established and worked out in details (this algebraic identity has a number of interpretations and implications in many branches of mathematical physics, and we will briefly review some of them in the concluding remarks). In this section it will be recognized how the BE identity complies with the two projective Desargues spin networks viewed, on the one hand, as a collection of five nested quadrangles, and as associated to the 4-simplex on the other. Such an algebraic setting can be further improved by calling into play Regge symmetry of the $6j$ symbol [20], previously discovered for the Wigner $3j$ symbol [21]. The prominent feature of Regge symmetry is its functional, not geometric origin, grounded into the Racah sum rule for the $6j$ symbol, *cf.* [22, 23] for reviews and original references. However, over the years it has been recognized as multi–faceted and still intriguing in many respects, ranging from its interpretation as non trivial automorphism group of a set of not-congruent Euclidean tetrahedra [24], up to its relation with Okamoto symmetry of the Painlevé VI differential equation [25]. We have been working on the aspects related to quadratic operator algebras, a frame that includes general (binary and symmetric) recoupling theory of $SU(2)$ angular momenta, as well as on the semiclassical analysis of three–term recursion relations, *cf.* [12, 13] also for a complete list of

references. The definition of Regge symmetry is briefly reviewed at the beginning of the section, and it will be shown that, by suitably ordering and keeping fixed the spin labels assigned to the four edges of a given reference quadrangle, the quantum amplitude of each Desargues spin network is automatically regularized in terms of a positive integer as happens when working *ab initio* within the framework of representation theory of the quantum group $SU(2)_q$ at $q = \text{root of unity}$ [26, 27].

In section 4 a glimpse to other interconnections and further developments will be addressed.

2. Desargues spin networks

In this section we are going to present a novel hierarchical construction of projective spin networks, from an assembling of five quadrangles up to the combinatorial 4-simplex (5 vertices, 10 edges, 10 triangular faces, 5 tetrahedra) compatible with a geometrical *realization* in Euclidean 4-space. We proceed in parallel and consistently with ‘combinatorial’ labeling of configurations, on the one hand, and with labeling provided by angular momentum theory, on the other. The algebraic content of the construction, together with an improved regularization procedure, are addressed in section 3. We refer to appendices 5.1 and 5.2 for a primer on angular momentum (re)coupling theory and for the discussion of the projective features of the configurations and diagrams of this section. Notations and conventions are those of the classic handbook [23].

2.1. Combinatorics of nested quadrangles

The basic building block of the construction is the $6j$ symbol presented through its Yutsis diagram as in Fig.1 or, equivalently, as the complete quadrangle of Fig.15, where $(a, b, c, d, x, y) \in \{0, 1/2, 1, 3/2, \dots\}$ label irreducible representations (*irreps*) of the Lie group $SU(2)$.

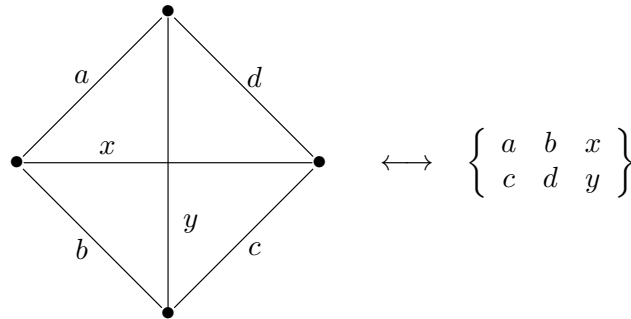


Figure 1. The Yutsis diagram of the $6j$.

The Desargues configuration $(10)_3$ shown in Fig.2 –the symmetric incidence structure made of ten points and ten lines– turns out to be combinatorially consistent with an assembling of five quadrangles, \mathcal{Q}_1 , \mathcal{Q}_2 , \mathcal{Q}_3 , \mathcal{Q}_4 and \mathcal{Q}_5 , in one-to-one correspondence with the coloring (Black, Red, Blue, Purple, Green). The ten bubbles which stand at the intersection of three lines are 3-valent vertices and have a double (unordered) labeling since each of them is shared by two quadrangles. The six edges of each quadrangle inherit colors from (one of) the colors of vertices. The angular momentum (spin) labeling of the five quadrangles –to be associated with the five $6j$ symbols of the BE identity in the following section– is depicted in Fig.3 and is given by the correspondences

$$\mathcal{Q}_1 \leftrightarrow \begin{Bmatrix} a & b & x \\ c & d & p \end{Bmatrix}; \mathcal{Q}_2 \leftrightarrow \begin{Bmatrix} c & d & x \\ e & f & q \end{Bmatrix}; \mathcal{Q}_3 \leftrightarrow \begin{Bmatrix} e & f & x \\ b & a & r \end{Bmatrix}; \mathcal{Q}_4 \leftrightarrow \begin{Bmatrix} p & q & r \\ f & b & c \end{Bmatrix}; \mathcal{Q}_5 \leftrightarrow \begin{Bmatrix} p & q & r \\ e & a & d \end{Bmatrix}. \quad (1)$$

It is worth pointing out that now the incidence structure underlying Desargues configuration has to be thought of as *geometrically* realized in a 3D projective or Euclidean space (namely the perspective point of Desargues' Theorem must be in general position with respect to the planes of the two triangles, cf. Fig.18). In a 3D Euclidean space, in particular, the five quadrangles considered so far would appear nested into each other, and not glued to each other to form a polyhedron. However, the duality principle (appendix 5.2) can be called into play to establish the actual existence of the space-dual of Desargues configuration, which will be proven below to be compatible not only with a combinatorial 4-simplex as noted in [2, 28], but also with a spin labeling of the 4-simplex.

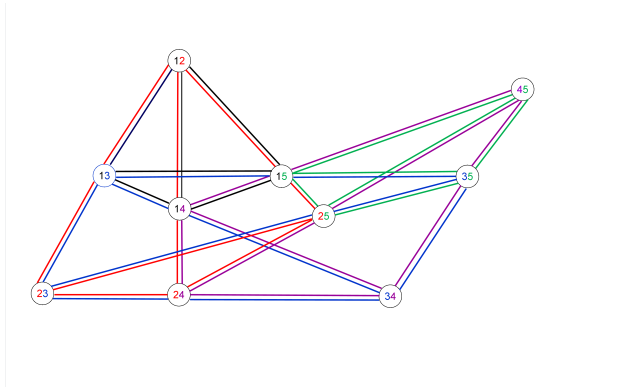


Figure 2. Combinatorial labeling of Desargues configuration $(10)_3$.

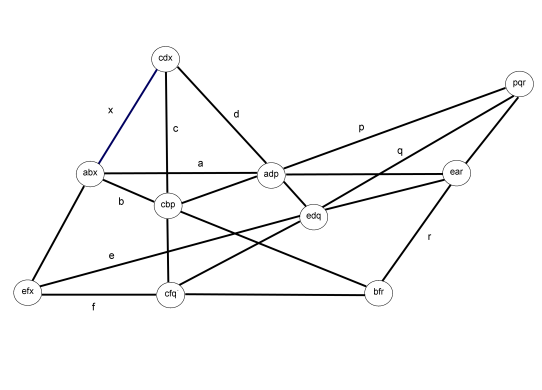


Figure 3. Spin labeling of Desargues configuration $(10)_3$.

2.2. Space-dual of Desargues configuration and the 4-simplex

The notion of duality applies in a straightforward way to the combinatorial labeling used in Fig.2. The points are two-colored, denoted by circles or round brackets, (12), (23), ...; quadrangles are listed 1, 2, 3, 4, 5 as in Eq.(1); lines are enumerated by triples of points, e.g. (12) (13) (23). An intermediate step consists in switching the line labeling to the dual one, where for instance the previous line is labeled with the two complementary colors [45] within square brackets, see all the resulting tags in Fig.4.

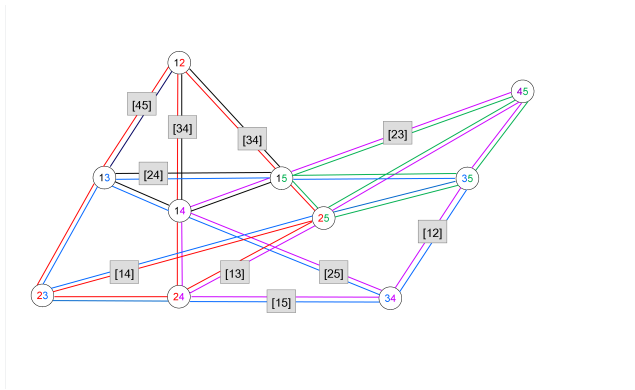


Figure 4. Dual labeling of lines put on top of Desargues configuration of Fig.2.

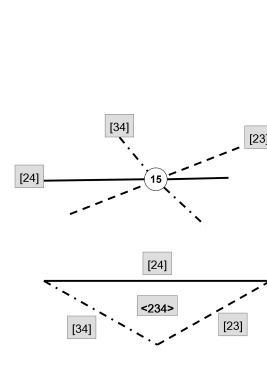


Figure 5. A blown-up 3-valent vertex and its dual triangle.

Recall from the final part of appendix 5.2 that in a projective space P^3 there is duality between subspaces of dimension k and $(3 - k - 1)$ and then the basic correspondences for going through the space–dual of Desargues configuration (theorem) are

$$\begin{aligned} \text{point} &\longrightarrow \text{plane}, \\ \text{line} &\longrightarrow \text{line}, \\ \text{quadrangle} &\longrightarrow \text{point}, \end{aligned}$$

where the last pairing can be worked out starting from the dualization of labeling of the original quadrangles, *e.g.* $\mathcal{Q}_1 \rightarrow \text{vertex } \{2345\}$ (curly brackets) in the space–dual configuration. Moreover, noting that the intersections of pairs of quadrangles represent the vertices of the original configuration of Fig.2, namely

$$\mathcal{Q}_i \cap \mathcal{Q}_j = (ij), \quad i, j = 1, 2, 3, 4, 5 \text{ with } i \neq j, \quad (2)$$

and recalling that any such vertex is actually the intersection of three lines (a *triad* of spin labeling according to the dictionary of Fig.3), we are forced to improve the duality (point \rightarrow plane) as

$$3\text{-valent vertex} \longrightarrow \text{triangle}$$

and to assign the combinatorial labels according to

$$2\text{-color vertex}(ij) \rightarrow \text{triangle } \langle klm \rangle \quad (3)$$

with k, l, m complementary to (ij) , *cf.* Fig.5.

The statement of the space–dual of Desargues’ theorem reads:

If two trihedra in 3D space are perspective from a triangle, then there exists a line connecting the tips of the two trihedra together with three planes meeting at this line and passing through the sides of the triangle.

The resulting connected ensemble of five vertices, ten lines, ten triangles and five tetrahedra (actually trihedra, each pair of which intersects a fourth triangle) is combinatorially a 4-simplex, denoted \mathcal{S}_{comb} for short. The pictorial representation of this construction is given in Fig.6 where the quadrangles \mathcal{Q}_1 and \mathcal{Q}_5 –or, respectively, dual vertices $\{2345\}$ and $\{1234\}$ – have been employed consistently with the choice made in Fig. 5 (actually any other choice of the selected pair of quadrangles turns out to be combinatorially equivalent to each other).

As for spin labeling of this new configuration, observe preliminary that the dual combinatorial labels on edges established in Fig.4 have been retained also for lines in the dual Desargues configuration on the basis of the duality (line \rightarrow line) in space. Thus, by resorting to the dictionary of Fig.3, and denoting the five tetrahedra of the combinatorial 4-simplex \mathcal{S}_{comb} by \mathcal{T}_i , the correspondence with $6j$ symbols arranged into the upgraded \mathcal{S}_{spin} , is necessarily given by

$$\mathcal{T}_1 \leftrightarrow \begin{Bmatrix} a & b & x \\ c & d & p \end{Bmatrix}; \mathcal{T}_2 \leftrightarrow \begin{Bmatrix} c & d & x \\ e & f & q \end{Bmatrix}; \mathcal{T}_3 \leftrightarrow \begin{Bmatrix} e & f & x \\ b & a & r \end{Bmatrix}; \mathcal{T}_4 \leftrightarrow \begin{Bmatrix} p & q & r \\ f & b & c \end{Bmatrix}; \mathcal{T}_5 \leftrightarrow \begin{Bmatrix} p & q & r \\ e & a & d \end{Bmatrix}. \quad (4)$$

The crucial difference with respect to the correspondence between quadrangles of the original Desargues configuration and $6j$ ’s given in (1) consists in recognizing that here the triads of the $6j$ have to be assigned to the triangular faces of tetrahedra as a consequence of the appropriate *projective duality* stated in Eq. (3). As mentioned in appendix 5.1 such a presentation of the $6j$ stands at the basis of Ponzano–Regge model for (the semiclassical analysis of) 3D Euclidean gravity, where the spin labels of $SU(2)$ *irreps* are the weights assigned to edges and give rise to the discrete analog of the gravitational path integral measure on the metrics. An exploded view of the space–dual Desargues spin network \mathcal{S}_{spin} is shown in Fig. 7.

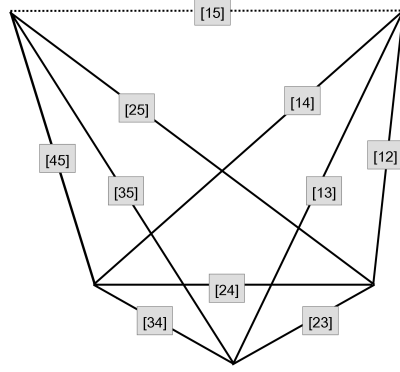


Figure 6. Space-dual of Desargues' theorem. Here the combinatorial labeling is only on lines for simplicity, but the labels of the other substructures are easily reconstructed from it: the two trihedra are incident on the triangle $\langle 234 \rangle = [23] \cup [24] \cup [34]$; the three planes of each trihedron are spanned by the three (of course not coplanar) lines $[25], [35], [45]$ and $[12], [13], [15]$, respectively; the theorem ensure the existence of line $[15]$ and of three planes (triangles) $\langle 125 \rangle$, $\langle 135 \rangle$, $\langle 145 \rangle$. The two vertices on the top represent the tips of the trihedra, labeled $\{2345\}$ and $\{1234\}$ or, by resorting again to complementarity of labeling, denoted 1 and 5, respectively.

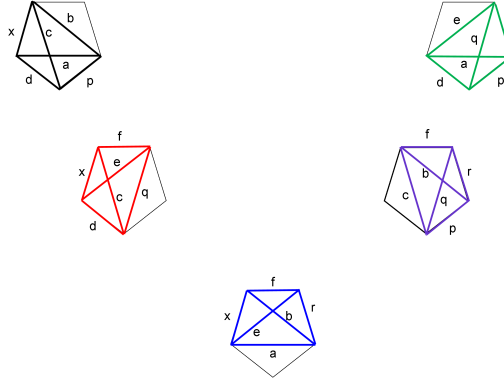


Figure 7. Spin labeling of the tetrahedra of the 4-simplex \mathcal{S}_{spin} : $(\mathcal{T}_1, \mathcal{T}_2, \mathcal{T}_3, \mathcal{T}_4, \mathcal{T}_5) \leftrightarrow (\text{Black, Red, Blue, Purple, Green})$, from top left in anti-clockwise order.

2.3. Geometrical realizations and dimensional reduction and increase

As already pointed out at the end of section 2.1, the hierarchical construction that leads to the Desargues spin network \mathcal{S}_{spin} discussed in section 2.2 (complemented with material of appendices 5.1 and 5.2) relies on the assumption that the underlying incidence structures are realized in a P^n with $n \geq 3$. The projective viewpoint provides, on the one hand, an axiomatic frame for dealing with incidence structures that *emerge* from the simplest configurations of points and lines in the plane, and an effective procedure based on projective *dimensional reductions* to go from the geometric realization of a 4-simplex in Euclidean space down to its low-dimensional cross-sections, on the other. The lines of reasoning underlying these achievements are summarized in

the following steps.

- Any two distinct points are incident with just a line and any two lines are incident with at least one point, (Axioms I) and II) of appendix 5.2). The existence of quadrangles (configurations $(4_3, 6_2)$) is the third axiom of (plane) projective geometry;
- Among the various finite configurations of points and lines, Desargues' (10_3) has a special status: in $n = 2$ it must be postulated separately but it is encoded as a theorem for $n \geq 3$, so that in the latter cases no further axiom is necessary;
- In $n = 3$ there exist two projective-dual versions of the theorem: its plane-dual, still denoted (10_3) because the configuration is symmetric under the exchange (points \leftrightarrow lines), and its space-dual, denoted \mathcal{S}_{comb} , discussed at length in section 2.2;
- \mathcal{S}_{comb} can be realized through the projection of an Euclidean 4-simplex onto P^3 ;
- If we slice any such Euclidean realization of \mathcal{S}_{comb} by an arbitrary solid, each line is cut by this portion of space in a point, each plane in a line and each tetrahedron in a plane so that any cross-section of \mathcal{S}_{comb} represents a figure made of ten points, ten lines and five planes, namely Desargues' (10_3) [28].

Obviously the previous remarks touch basic questions about the nature of quantum spacetime, the existence of a fundamental length and a number of questions that arise in connection with discretized, simplicial or spin networks, approaches to quantum gravity, not to mention the issue of dimensional reduction [29]. Our view is inspired by the (quite elementary) frame provided by projective geometry of configurations and by its intriguing relations with angular momentum theory –relations that have been only partially worked out by other authors, sometimes leading to ambiguous conclusions, *cf.* the appendices.

The result we have been proving,

the Desargues configuration and its space-dual are respectively cross-sections and projections of an Euclidean 4-simplex, and consistent $SU(2)$ spin labeling can be assigned to each of them,

leaves open the crucial question of the existence of a ‘quantum of space’ in (space or spacetime) dimensions $D=3,4$. In the light of the previous considerations, one might either *i)* postulate the existence of an Euclidean 4-simplex, assign projective coordinates and go down to a 3D Desargues configuration which admits a spin labeling as in Fig.3, or *ii)* look for an emergent 3D (projective) space from the (re)coupling of angular momenta. The latter option is actually what occurs according to the combined results found by Penrose [5] and by Ponzano and Regge [4] which stand at the basis of all of the spin networks models addressed over the years in quantum gravity *cf.* [6, 18] for brief accounts and [9] for an extended overview on the Loop approach. Then the rationale of our construction relies on *ii)* and exploits the projective nature of the $SU(2)$ spin networks up to the emergency of the 4-simplex \mathcal{S}_{spin} .

3. Regge symmetry and improved algebraic setting

As is well known the defining relations for $6j$ symbols of $SU(2)$ are the orthogonality condition,

$$\sum_x (2x+1) \begin{Bmatrix} a & b & x \\ c & d & y \end{Bmatrix} \begin{Bmatrix} c & d & x \\ a & b & y' \end{Bmatrix} = \frac{\delta_{yy'}}{2y'+1} \delta_{(ady)} \delta_{(bcy)}, \quad (5)$$

where the symbol $\delta_{(\dots)}$ constrains the entries to belong to a triad, and the Biedenharn–Elliot (BE) identity

$$\sum_x (-1)^{\varphi+x} \begin{Bmatrix} a & b & x \\ c & d & p \end{Bmatrix} \begin{Bmatrix} c & d & x \\ e & f & q \end{Bmatrix} \begin{Bmatrix} e & f & x \\ b & a & r \end{Bmatrix} = \begin{Bmatrix} p & q & r \\ f & b & c \end{Bmatrix} \begin{Bmatrix} p & q & r \\ e & a & d \end{Bmatrix}, \quad (6)$$

where $\varphi = a + b + c + d + e + f + p + q + r$. The content of this algebraic relation, depicted in Fig.8, complies with the assignments of spin labels/triads to lines/vertices –resulting in the association $6j \leftrightarrow$ quadrangles (see Eq.(1))– in the Desargues configuration $(10)_3$ as established in Fig.3.

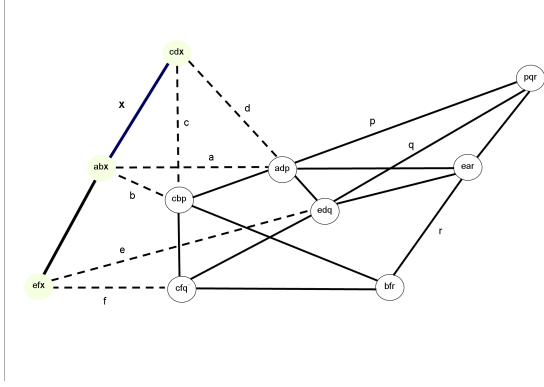


Figure 8. Upon summation over x (bold), three triads of spin labels together with the dashed edges disappear: only the two quadrangles corresponding to the $6j$'s on the right side of the BE identity survive.

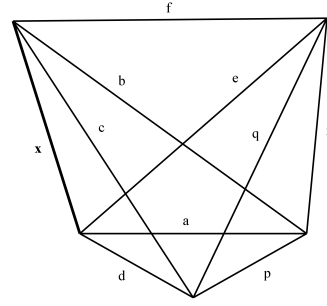


Figure 9. The BE identity in the Desargues space-dual \mathcal{S}_{spin} model: here labelings are identical to those of Fig.7.

On the other hand, *the same spin assignment* turns out to be compatible with the 4-simplex frame \mathcal{S}_{spin} associated with the space-dual of Desargues configuration discussed at length in section 2.2, and the BE identity holds true consistently, *cf.* Fig. 9. In other words, the geometric content of the BE identity in the Ponzano–Regge tetrahedral presentation of the $6j$ (see appendix 5.1) is intrinsically projective, as far as the two arrangements (3 tetrahedra joined along x) and (two tetrahedra joined along one common face) cannot coexist in an Euclidean 3-space but can be realized through \mathcal{S}_{spin} in dimension 4. The latter remark holds true for the coexistence of the arrangements (4 tetrahedra joined together and incident on a common vertex) and (1 tetrahedron) which would correspond to an identity easily derived from (6) by resorting to (5)). In Fig.10 and Fig.11 the purely topological versions of the so-called Pachner moves [30] for simplicial 3-manifolds are depicted.

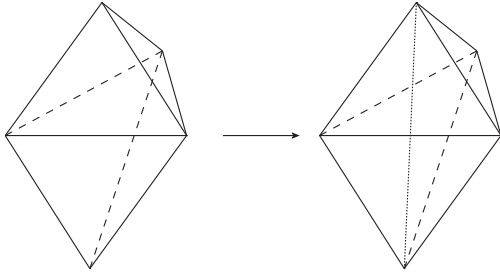


Figure 10. Pachner move 2-3

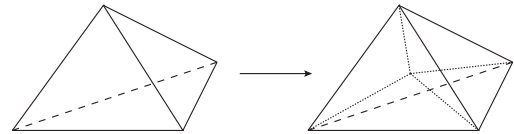


Figure 11. Pachner move 1-4

Looking back at the $6j$ symbol of Fig.1, the four labels (a, b, c, d) –associated with the consecutive sides of a quadrangle, or equivalently of a tetrahedron *cf.* 5.1– are going to be treated as tunable parameters, while $\begin{pmatrix} x \\ y \end{pmatrix}$ is thought of as the pair of variables corresponding

to the matrix indexes of the $6j$ when applied to binary coupled states of three $SU(2)$ angular momenta in the space of the total angular momentum [23]. As is well known the 24 ‘classical’ symmetries of the $6j$ can be viewed geometrically as associated to the complete tetrahedral group (isomorphic to S_4) and leave the (values of the) symbol invariant under any permutation of its columns or under interchange of the lower and upper arguments in each of any two columns. The Regge symmetries [20] are expressed as functional relations among parameters and read

$$\begin{Bmatrix} a & b & x \\ c & d & y \end{Bmatrix} = \begin{Bmatrix} s-a & s-b & x \\ s-c & s-d & y \end{Bmatrix} := \begin{Bmatrix} a' & b' & x \\ c' & d' & y \end{Bmatrix}, \quad (7)$$

where $s := (a + b + c + d)/2$ is the semi-perimeter of the quadrangle and in the last equality the new set (a', b', c', d') is defined. The $6j$ associated with the primed entries represents the Regge ‘conjugate’ of the original quadrangle, and of the Ponzano–Regge tetrahedron as well. Combining the symmetries given in (7) with two more sets obtained by keeping the other pairs of opposite entries fixed, it turns out that the total number of symmetries is 144, which equals the order of the product permutation group $S_3 \times S_4$.

In the $6js$ of Eq.(7) the range of the running entries is $x_{max} - x_{min} = y_{max} - y_{min} = 2 \min(a, b, c, d, a', b', c', d')$ on the basis of the choice of a particularly useful ordering for dealing with the discrete, four-parameter $6j$ -function, see [12, 13]. This construction highlights in particular ‘Regge-invariant’ geometric realizations of both quadrangles and tetrahedra, a symmetry which naturally extends to the three-term recursion relations which hold for the $6j$ symbol [23, 31], on the one hand, and for eigenfunctions of the volume operator, on the other [11, 14].

Here we just add a remark about the role Regge symmetry in providing a natural regularization on the representation ring of $SU(2)$, once the set of spins a, b, c, d (and thus the semi-perimeter s) is kept fixed. If we denote a the smallest among the eight (integer and semi-integer) parameters $(a, b, c, d, s-a, s-b, s-c, s-d)$, then we assign the label c to the opposite entry, cf. the first $6j$ in (7), and d is chosen as the biggest among the two remaining labels. The ordering and the range of c which turn out to be compatible with all of the quadrangular and triangular inequalities are given by

$$a \leq b \leq d \leq s; \quad d - (b - a) \leq c \leq d + (b - a) \quad (8)$$

and $x_{max} - x_{min} = y_{max} - y_{min} = 2a$. It is easily checked that the semi-perimeter s satisfies

$$s \leq \max\{a, b, c, d\} \equiv d + (b - a), \quad (9)$$

a condition to be compared with what would happen for the $SU(2)_q$ case with q a root of unity. The following inequality, proven explicitly in [32] and adapted here to our conventions on spin labeling,

$$s \leq \min\{a, b, c, d\} + \frac{(r-2)}{2} := a + \kappa, \quad (10)$$

involves the integer $r \geq 3$ with $q = e^{2\pi i/r}$. The two inequalities above lead to the compatibility condition

$$\kappa \leq x_{min} + y_{min} \quad \text{or} \quad r \leq (2x_{min} + 1) + (2y_{min} + 1), \quad (11)$$

interpreted as associated with a sort of effective q -regularization. The integer r is thus bounded by the sum of the dimensions of the $SU(2)$ irreps labeled x_{min}, y_{min} and the geometrical content of Eq.11 relies on the identification of x_{min}, y_{min} with the lower admissible values of the lengths of the diagonals of the quadrangle in Fig.15 or of two opposite edges in the solid Euclidean tetrahedron in Fig.16 of Appendix 5.1. It is worth noting that, owing to the nested structure of the quintuple of quadrangles, it can be easily shown that the regularization conditions above can be fixed on a single reference quadrangle (or even on a single tetrahedron in \mathcal{S}_{spin}).

A quite interesting reformulation of the remarks presented so far would be in term of a quaternionic reparametrization of the entries of the $6j$ as given in Eq.7: the semi-perimeter

s represent the real part of a quaternion \mathfrak{Q} and three independent linear combinations of (a, b, c, d) give its other real components. Then it turns out that the Regge-transformed $6j$ is associated with the ‘conjugate’ \mathfrak{Q}' of quaternion \mathfrak{Q} , a circumstance that justifies algebraically the use of term ‘Regge–conjugate’ for the $6j$ on the right side of Eq.7 (note that octonions should also be called into play as consistent coordinatization of pairs $(\mathfrak{Q}, \mathfrak{Q}')$). More details on such a reparametrization, its implications and a few applications can be found in [12, 13].

4. Outlook and conclusions

Actually quite a lot of issues and interconnections have not been addressed here for lack of space. As for the BE identity, recall that it has been used originally for proving the combinatorial invariance of the Ponzano–Regge state sum under refinement, *cf.* the moves depicted in Fig.10 and Fig.11. In the same paper it can be found the derivation of the three-term recursion relation for the $6j$ symbol that in the semiclassical limit (where all angular momentum variables are much greater than 1 in \hbar units) gives the asymptotic formula for the $6j$. As mentioned already in the introduction, this model has been extensively used in discrete quantum gravity approaches, as well as in topological quantum computing see [33, 34, 35, 36]. Of particular interest in quantum gravity applications is the volume operator of the tetrahedron: on the basis of the paper [11] we have developed recently a complete analysis of the three-term recursion relation for the eigenfunctions of such operator highlighting the proper Regge–invariant frame of Racah quadratic algebra [37, 38, 14], as well as the emergence of a Hamiltonian dynamics at the classical level [12].

In summary, we have emphasized in the present paper the central role played in Regge–regularized Desargues spin networks by the BE identity (together with the orthogonality relation) as the common algebraic counterpart of assemblings of quintuples of projectively–related quadrangles and tetrahedra, as well as of the associated geometric realizations. As for dimensional reduction through projections from 3D to 2D and 1D of Desargues spin networks, we argue that it should be possible to proceed in parallel with semiclassical limiting procedures achieved by taking suitable partial limits of the three–term recursions for the $6j$ symbol and for the volume operator quoted above. The level of persistence of Regge symmetry might represent a guiding principle in this kind of analysis. Finally, as for the 4-simplex – realized through the space-dual of a Desargues spin network – we have shown in section 2.3 how its 3D cross sections still represents the (original) Desargues spin network, thus opening the possibility of looking at dimensional reduction from 4D to 3D in a new perspective. We argue also that, by properly framing the projective tools within a picture grounded into recursion relationships governed by discrete variables, a Hamiltonian description for the amplitude of the 4-simplex might emerge. Work is in progress in this direction.

5. Appendix: Projective configurations and angular momentum theory

5.1. The triangle of couplings and the quadrangle of recouplings

Triangular inequalities involving three *irreps* labels of $SU(2)$ angular momenta basically arise from the Clebsch–Gordan series, $\mathcal{H}^{j_1} \otimes \mathcal{H}^{j_2} = \bigoplus_{j=|j_1-j_2|}^{j_1+j_2} \mathcal{H}^j$, where \mathcal{H}^j is the $(2j+1)$ –dimensional Hilbert space of the (square of the) total angular momentum \mathbf{J} ($-j \leq m \leq j$) with m being the magnetic quantum number associated with J_z , the component of \mathbf{J} along the quantization axis. The two independent systems of sharp angular momenta \mathbf{J}_1 and \mathbf{J}_2 have dimensions satisfying $(2j_1+1)(2j_2+1) = (2j+1)$ and the (orthogonal) transformation between the basis vectors of $\mathcal{H}^{j_1} \otimes \mathcal{H}^{j_2}$ and those of \mathcal{H}^j is given by Clebsch–Gordan coefficients or by their symmetrized counterpart, the Wigner $3j$ symbol $\begin{pmatrix} j_1 & j_2 & j \\ m_1 & m_2 & m \end{pmatrix}$ with $m_1 + m_2 = m$. Such an unordered triple of angular momentum variables (spins), say (j, k, l) taking values in $\{0, 1/2, 1, 3/2, \dots\}$, constitutes a *triad* and can be graphically represented as either a trivalent vertex (Fig.12), or as a triangle (Fig.13), or else by three points lying on a same line (Fig. 14). The latter was first noticed

by Fano and Racah [3], hence unveiling the intriguing connection between (binary) coupling of angular momenta and (finite) projective configurations of points and lines discussed below.

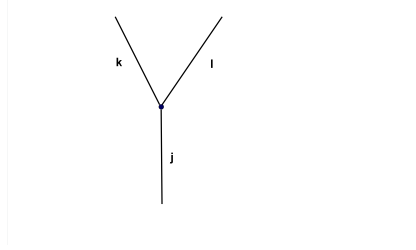


Figure 12. The triad (j, k, l) associated with a trivalent vertex.

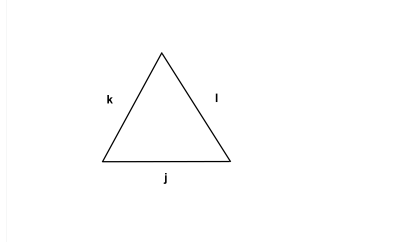


Figure 13. The triad (j, k, l) associated with a triangle.

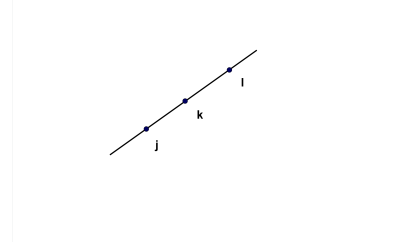


Figure 14. The triad (j, k, l) associated with three points on a same line.

The basic building block of angular momentum theory is the W recoupling coefficient of Racah or, equivalently, the Wigner $6j$ symbol ($a, b, c, d, x, y \in \{0, 1/2, 1, \dots\}$)

$$\left\{ \begin{matrix} a & b & x \\ c & d & y \end{matrix} \right\} \text{ with triads } (abx), (bcy), (cdx), (ady) \quad (12)$$

As is well known there exist three alternative graphical presentations of the combinatorial content of this symbol, discussed below focusing on their interpretations in projective geometry.

The $6j$ as a complete quadrangle (Fig.15)

Edmonds [39] showed that the $6j$ –together with other recoupling coefficients such as the $9j$ and the $12j$ symbols– can be associated with trivalent graphs obtained by joining the free ends of binary coupling trees whose labeling are consistent with that of the trivalent vertex of Fig.12. On this basis Yutsis and collaborators [10] elaborated a general diagrammatical scheme able to work out complicated calculations –involving generalized Clebsch–Gordan coefficients and $3nj$ recoupling coefficients– by resorting to combinatorial operations on such labeled graphs. An upgraded version of these methods is collected in the handbook by Varshalovich and collaborators [23], the notation of which is used thoroughly in this paper. In particular, the $6j$ is depicted as a complete graph on four vertices as in Fig.1, each vertex being associated with a triad of spin labels. Notably, when each edge is extended to a line, the resulting configuration can be perceived projectively as a *complete quadrangle*, denoted $(4_3, 6_2)$.

The $6j$ as a tetrahedron (Fig.16)

The second graphical presentation dates back to Wigner [40] and Ponzano and Regge [4] and has been especially exploited in connection with the semiclassical limit of the $6j$ symbol representing an Euclidean tetrahedron in the classically allowed region where its square volume is positive. Here spin labels are associated with the edge lengths and the triads with the triangular faces as in Fig.13. The relationship between the two presentations –quadrangle and tetrahedron– is easily recognized in polyhedral geometry: if the quadrangle of Fig.15 is realized in Euclidean 3-space as a tetrahedron (with the condition on the volume given above), or, equivalently, if it represents the projection on a plane of a solid tetrahedron, then under topological duality of 2D simplicial complexes, (vertex \leftrightarrow triangle) and (edge \leftrightarrow edge), the two diagrammatical presentations are turned into each other. (Obviously this correspondence involves the triangulation of the boundary of the tetrahedron while in the study of 3D simplicial dissections of manifolds most of the results and applications rely on the duality (0-simplex \leftrightarrow 3-simplex) and (1-simplex \leftrightarrow 2-simplex)).

The $6j$ as a complete quadrilateral (Fig.17)

This presentation, derived from the assignment (triad \leftrightarrow three points on a line) of Fig.14, has

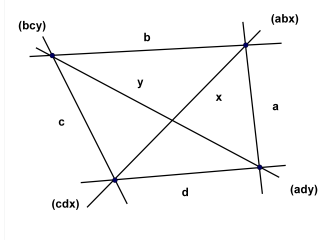


Figure 15. The configuration $(4_3, 6_2)$: four points in a plane are joined in pairs by six distinct lines.

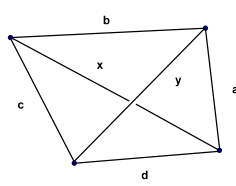


Figure 16. The tetrahedron (the boundary of a 3-simplex) has four vertices, six edges and four triangular faces.

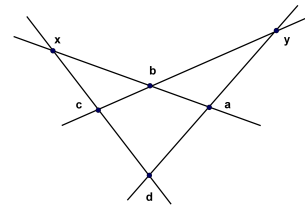


Figure 17. The configuration $(6_2, 4_3)$: four lines in a plane meet by pairs in six distinct points.

been the basic tool to disclose the projective content of angular momentum recoupling theory since Fano and Racah. We refer the reader interested in more details to the papers of Robinson [41], Judd [42], Labarthe [43] and to the book of Biedenharn and Louck [22]. The quadrangle of Fig.15 is related to the quadrilateral by the standard projective duality in the plane, (point \leftrightarrow line).

It is worth to remark that it is actually the configuration (7_3) of seven points and seven lines (known as the Fano plane) that historically has attracted much attention, and has been also the object of recent investigations by the authors in connection with applications to atomic and molecular physics, *cf.* [44] and references therein.

5.2. Assembling of projective configurations: from quadrangles to Desargues configuration

The three presentations of the $6j$ symbol (12) –two of which are truly projective configurations as recognized above– have been used alternately in different approaches to quantum spin networks, even though from the combinatorial viewpoint they are related by simple (projective or Poincaré) duality transformations as pointed out above. Taken for granted that each of them matches with the standard algebraic setting (in particular with the three-term recursion relation for the $6j$ [23]), we are implementing a bottom-up approach to construct spin networks from the basic axioms of projective geometry (as stated in [1]) and showing how assembling quadrangles – rather than quadrilaterals– turns out to be the most economical and consistent way of looking at emergent geometric realizations of interest also in discretized quantum gravity models, *cf.* the final remarks at the end of section 2.3. The first two incidence axioms are

I) Any two distinct points are incident with just a line.

II) Any two lines are incident with at least one point.

A configuration in the plane is denoted (p_γ, ℓ_π) , where p is the number of points, ℓ the number of lines, γ the number of lines per point, and π the number of points per line. The equality $p\gamma = \ell\pi$ is easily verified, and configurations for which $p = \ell$ and $\gamma = \pi$, so that $(p_\gamma, p_\gamma) \equiv (p_\gamma)$, are called symmetric (for instance (3_2) is a triangle and (n_2) a polygon with n sides). The (standard) projective dual to a configuration (p_γ, ℓ_π) is a configuration (ℓ_π, p_γ) in which the roles of points and lines are interchanged, and symmetric configurations are self-dual in the plane by definition. The complete quadrangle $(4_3, 6_2)$ of Fig.15 and quadrilateral $(6_2, 4_3)$ of Fig.17 are dual to each other, as already noted. The existence of the quadrangle bears on the axiom

III) There exist four points, no three of which are collinear.

Actually this is the simplest configuration that allows for the assignment of coordinates in the plane, looking at the complete quadrangle $(4_3, 6_2)$ of Fig. 15 with vertices labeled by the pairs $(0,0)$ $(0,1)$ $(1,0)$ $(1,1)$ taking values in the smallest finite number field \mathbb{F}_2 [45].

Focusing on symmetric configurations, it should be clear that the symbolic expression (p_γ) does not determine uniquely a projective configuration up to incidence isomorphisms. In particular, among the ten different (10_3) configurations, the Desargues configuration plays a prominent role in projective geometry essentially because it encodes Desargue's theorem. The statement is illustrated in Fig.18. Actually Desargues' theorem holds true in any projective

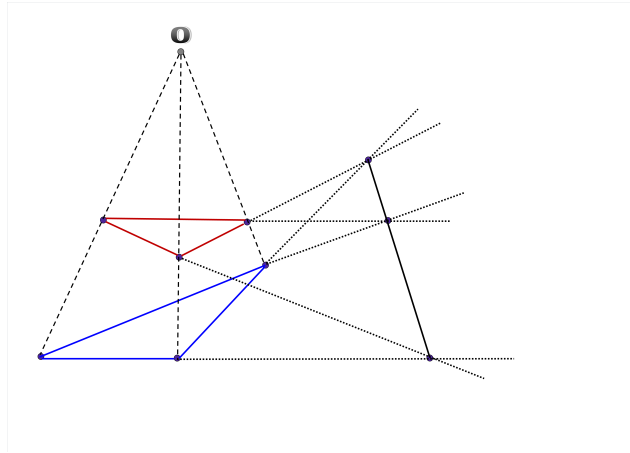


Figure 18. Illustration of Desargues' theorem: if two triangles (red and blue) are in perspective from a center O , then the extensions to lines of their sides meet in a line, the perspective line. In the (plane) dual of this theorem the existence of the perspective line with three points is assumed and the existence of the center of perspective O is proven.

geometry P^n for $n \geq 3$ while its realization in the plane P^2 must be separately postulated (cf. [1]). The principle that characterizes projective geometry and is crucial for the hierarchical construction of spin networks is *duality* (the notion of plane duality, or duality in P^2 , has been already quoted above). In general, suppose that in a proposition –or a figure, or a configuration– in P^n one interchanges P^n and P^{n-r-1} ($0 \leq r \leq n$) and switches ‘is contained’/ ‘contains’, ‘collinear’/ ‘concurrent’ and similar. Then the duality principle can be stated as follows

Duality principle. If a proposition (about a configuration) is true in P^n then it is also true in *any of the dual configurations* of the original one lying in P^{n-r-1} for $0 \leq r \leq n$.

References

- [1] Coxeter H S M 1974 *Projective Geometry* (Berlin: Springer-Verlag)
- [2] Hilbert D and Cohn-Vossen 1952 *Geometry and the Imagination* (Chelsea: Amer. Math. Soc.)
- [3] Fano U and Racah G 1959 *Irreducible Tensorial Sets* (New York: Academic Press)
- [4] Ponzano G and Regge T 1968 *Semiclassical Limit of Racah Coefficients* in *Spectroscopic and Group Theoretical Methods in Physics* ed F Bloch et al (Amsterdam: North-Holland) pp 1-58
- [5] Penrose R 1971 *Angular Momentum: an Approach to Combinatorial Space-time* in *Quantum Theory and beyond* Bastin T ed (Cambridge: Cambridge University Press) pp 151-180
- [6] Carfora M, Marzuoli A and Rasetti M 2009 *J. Phys. Chem. A* **113** 15376
- [7] Carfora M and Marzuoli A 2012 *Quantum Triangulations: Moduli Spaces, Strings, and Quantum Computing* (Lect. Notes in Physics **845**) (Berlin: Springer-Verlag)
- [8] Rovelli C and Vidotto F 2017 *Covariant Loop Quantum Gravity: An Elementary Introduction To Quantum Gravity And Spinfoam Theory* (Cambridge: Cambridge University Press)
- [9] Ashtekar A and Pullin J 2017 *Loop Quantum Gravity: The First 30 Years* (Singapore: World Scientific)
- [10] Yutsis A, Levinson I, Vanagas V 1962 *Mathematical Apparatus of the Theory of Angular Momentum* (Israel Program of for Scientific Translation)
- [11] Carbone G, Carfora M and Marzuoli A 2002 *Class. Quantum Grav.* **19** 3761
- [12] Aquilanti V, Marinelli D and Marzuoli A 2013 *J. Phys. A: Math. Theor.* **46** 175303

- [13] Marinelli D 2013 *Single and Collective Dynamics of Discretized Geometries* PhD Thesis (Pavia, Italy: University Press) ISBN 978-88-95767-73-4
- [14] Aquilanti V, Marinelli D and Marzuoli A 2014 *J. Phys.: A: Conf. Series* **46** 175303
- [15] Ragni M, Bitencourt A C P, Da S Ferreira C, Aquilanti V, Anderson R W and Littlejohn R G 2010 *Int. J. Quantum Chem.* **110** 731
- [16] Aquilanti V, Haggard H M, Hedeman A, Jeevanjee N, Littlejohn R G and Liang Y 2012 *J. Phys. A: Math. Theor.* **45** 065209
- [17] Bitencourt A C P, Marzuoli A, Ragni M, Anderson R W and Aquilanti V 2012 *Lect. Notes Comput. Science* **7333** Part I ed B Murgante et al (Berlin Heidelberg: Springer-Verlag) p 723
- [18] Regge T and Williams R M *J. Math. Phys.* **41** 3964
- [19] Regge T 1961 *Nuovo Cim.* **19** 558
- [20] Regge T 1959 *Nuovo Cim.* **11** 116
- [21] Regge T 1958 *Nuovo Cim.* **10** 544
- [22] Biedenharn L C and Louck J D 1981 *The Racah-Wigner Algebra in Quantum Theory* (Encyclopedia of Mathematics and its Applications Vol 9) ed G-C Rota (Reading, MA: Addison-Wesley)
- [23] Varshalovich D A, Moskalev A N and Khersonskii V K 1988 *Quantum Theory of Angular Momentum* (Singapore: World Scientific)
- [24] Roberts J 1999 *Geom. Topology* **3** 21
- [25] Boalch P P 2007 *Commun. Math. Phys.* **276** 117
- [26] Biedenharn L C and Lohe M A 1995 *Quantum Group Symmetry and q-Tensor Algebra* (Singapore: World Scientific)
- [27] Koekoek R, Lesky P A and Swarttouw R F 2010 *Hypergeometric Orthogonal Polynomials and Their q-Analogues* (Heidelberg: Springer)
- [28] Barnes J 2012 *Gems of Geometry* (Heidelberg: Springer)
- [29] Carlip S 2012 *Spontaneous Dimensional Reduction? Preprint* 1207.4503 [gr-qc]
- [30] Pachner U 1991 *Eur. J. Combin.* **12** 129
- [31] Ragni M, Littlejohn R G, Bitencourt A C P, Aquilanti V and Anderson R W 2013 *Lect. Notes Comput. Science* **7972** (Berlin Heidelberg: Springer-Verlag) p 60
- [32] Khavkine I 2015 *Int. J. Geom. Meth. Mod. Phys.* **12** 1550117
- [33] Marzuoli A and Rasetti M 2005 *Ann. Phys.* **318** 345
- [34] Marzuoli A and Rasetti M 2002 *Phys. Lett. A* **306** 79
- [35] Garnerone S, Marzuoli A and Rasetti M 2009 *Adv. Theor. Math. Phys.* **13** 1601
- [36] Kádár Z, Marzuoli A and Rasetti M 2009 *Int. J. Quantum Inf.* **7** 195
- [37] Sklyanin E K 1982 *Funct. Anal.* **16** 263
- [38] Granovskii Ya I, Lutzenko I M and Zhedanov A S 1992 *Ann. Phys.* **217** 1
- [39] Edmonds A 1960 *Angular Momentum in Quantum Mechanics* (Princeton NJ: Princeton Univ. Press)
- [40] Wigner E 1959 *Group Theory and its Application to the Quantum Mechanics of Atomic Spectra* (New York: Academic Press)
- [41] Robinson deB G 1970 *J. Math. Phys.* **11** 3428
- [42] Judd B 1983 *Found. Phys.* **13** 51
- [43] Labarthe J-J 2000 *J. Phys. A* **13** 763
- [44] Santos R F, Arruda M S, Bitencourt A C P, Ragni M, Prudente F V, Coletti C, Marzuoli A and Aquilanti V 2017 *J. Mol. Spectrosc.* **337** 153
- [45] Hall M 1983 *Trans. Amer. Math. Soc.* **45** 229